

# IMPROVING ELECTRICITY GENERATION DURING PARTIAL SHADING BY ADJUSTING DUTY CYCLE IN MPPT USING IMAGE PROCESSING

Gunasekaran N<sup>1</sup>, Karthik T R<sup>2</sup>, Vijayalakshmi G<sup>3</sup>

<sup>1,2</sup> UG Student, Department of Electronics and Communication Engineering, Prince Shri Venkateshwara Padmavathy Engineering College, Tamilnadu, India

<sup>3</sup> Assistant professor, Department of Electronics and Communication Engineering, Prince Shri Venkateshwara Padmavathy Engineering College, Tamilnadu, India

## ABSTRACT

In today's modern world, increasing demand on electrical energy is high so solar energy is way to generate electrical energy. This paper deals with the image based cloud prediction approach which is proposed to adjust duty cycle of converter for maximum power. Due to the sun's path, the atmosphere's condition and the scattering process, the image is analyzed, then the duty cycle is changed by tracking maximum power point. Numerous applications are seeking to forecast irradiance and solar power as a range of solar generation technologies reach higher penetrations. The complex issues making solar forecasting necessary for optimal management of increasingly flexible modern electrical networks is discussed in this project. A sky-cam system and its application to managing solar energy in a mini-grids through predictive solar inverter and generator control.

**Keywords:-** Image processing, MPPT, Solar forecasting, Electrical energy.

## 1. INTRODUCTION

Sufficient supplies of maximum electrical energy from the solar panel is need. Tracking for maximum electrical energy can be achieved by using maximum power point tracking concept. By using a sky cam images analysis the sun position, the atmosphere's condition and the scattering process, then MPPT will identify the maximum power and generate energy. Solar photovoltaic systems transform solar energy into electric power. The output power depends on the incoming radiation and on the solar panel characteristics. Solar forecasts on multiple time horizons play an important role in storage management of PV systems, control systems in buildings, hospitals, schools etc., control of solar thermal power plants, as well as for the grids regulation and power scheduling. Solar forecasting can support residential, commercial and industrial solar thermal and photovoltaic plant design, operation and integration with local loads in order to maximize solar penetration and minimize grid import, export and energy costs.

### 1.1 MPPT

Maximum Power Point Tracking is algorithm that included in charge controllers used for extracting maximum available power from PV module under certain conditions. MPPT is efficient in the field of exploitation of renewable sources of energy. Maximum power point tracking is a DC-to-DC converter that optimizes the match between the solar array (PV modules) and the battery bank or utility grid. It converts a higher voltage DC output from solar PV arrays or modules down to the lower voltage needed to charge batteries and vice versa. Maximum Power Point Tracking is an electronic arrangement that routinely finds the voltage ( $V_{MPP}$ ) or current ( $I_{MPP}$ ) at which PV modules should operate to achieve maximum power output ( $P_{MPP}$ ) under partial shading condition.

## 1.2 SEPIC Converter

Power supply gives supply to all components. It is used to convert AC voltage into DC voltage. Transformer used to convert 230V into 12V AC. 12V AC is given to diode. Diode range is 1N4007, which is used to convert AC voltage into DC voltage. AC capacitor used to charge AC components and discharge on ground. LM 7805 regulator is used to maintain voltage as constant. Then signal will be given to next capacitor, which is used to filter unwanted AC component. Load will be LED and resistor. LED voltage is 1.75V. If voltage is above level beyond the limit, and then it will be dropped on resistor. Figure 4.4 shows the circuit diagram of the SEPIC converter which is used to store and discharge the charge. Fig - 1 shows the designed SEPIC converter in that the transformer is short circuited and it is converted in to inductor to store and discharge the charge to boost the power whenever the is low.

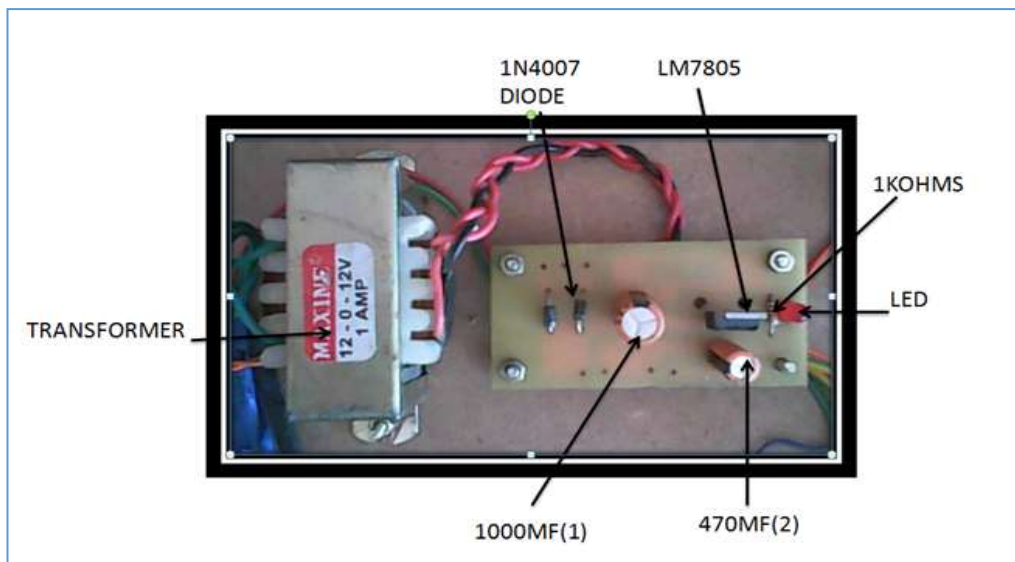


Fig -1: SEPIC Converter

## 2. IMAGE PROCESSING

Image-based forecasting techniques can make important contributions to short-term solar forecasting by identifying and predicting cloud movement and forecasting changes in solar availability. When combined with demand forecasting and storage or discretionary load control, a potent system for managing the supply–demand balance is established. Such a system enables a much more dynamic network operating range and potentially allows significantly more renewable energy to be integrated, while ensuring that sufficient generation and network capacity exists and that quality of supply is maintained. Even in the absence of demand forecasting and additional controllable elements, solar generation forecasting is becoming increasingly important to ensure that an efficient supply and demand balance is achieved as significant growth occurs in penetration of variable renewable generation. Refer the following steps of image processing in Fig-2.

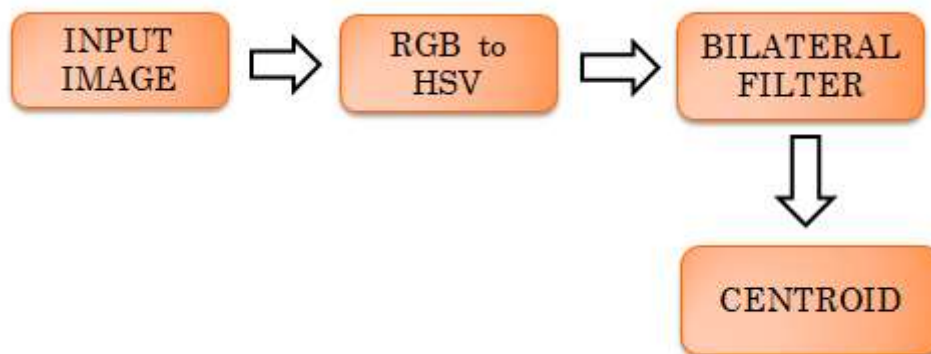


Fig -2: Image Processing Steps

## 2.1 RGB colour model

The RGB color model is an additive color model in which red, green and blue light are added together in various ways to reproduce a broad array of colors. The name of the model comes from the initials of the three additive primary colors, red, green, and blue. The main purpose of the RGB color model is for the sensing, representation and display of images in electronic systems, such as televisions and computers, though it has also been used in conventional photography. Before the electronic age, the RGB color model already had a solid theory behind it, based in human perception of colors. To form a color with RGB, three light beams (one red, one green, and one blue) must be superimposed (for example by emission from a black screen or by reflection from a white screen). Each of the three beams is called a component of that color, and each of them can have an arbitrary intensity, from fully off to fully on, in the mixture. The RGB color model is *additive* in the sense that the three light beams are added together, and their light spectra add, wavelength for wavelength, to make the final color's spectrum. This is essentially opposite to the subtractive color model that applies to paints, inks, dyes, and other substances whose color depends on *reflecting* the light under which we see them. Because of properties, these three colors create white, this is in stark contrast to physical colors, such as dyes which create black when mixed.

## 2.2 Converting from RGB to HSV

Color vision can be processed using RGB color space or HSV color space. RGB color space describes colors in terms of the amount of red, green, and blue present. HSV color space describes colors in terms of the Hue, Saturation, and Value. In situations where color description plays an integral role, the HSV color model is often preferred over the RGB model. The HSV model describes colors similarly to how the human eye tends to perceive color.

RGB defines color in terms of a combination of primary colors, where as, HSV describes color using more familiar comparisons such as color, vibrancy and brightness. The basketball robot uses HSV color space to process color vision. Hue represents the color type. It can be described in terms of an angle on the above circle. Although a circle contains 360 degrees of rotation, the hue value is normalized to a range from 0 to 255, with 0 being red. Saturation represents the vibrancy of the color. Its value ranges from 0 to 255.

The lower the saturation value, the more gray is present in the color, causing it to appear faded. Value represents the brightness of the color. It ranges from 0 to 255, with 0 being completely dark and 255 being fully bright. White has an HSV value of 0-255, 0-255, 255. Black has an HSV value of 0-255, 0-255, 0. The dominant description for black and white is the term, value. The hue and saturation level do not make a difference when value is at max or min intensity level. The color camera, on the robot, uses the RGB model to determine color. Once the camera has read these values, they are converted to HSV values. The HSV values are then used in the code to determine the location of a specific object/color for which the robot is searching. The pixels are individually checked to determine if they match a predetermined color threshold.

## 2.3 Bilateral filter

A bilateral filter is a non-linear, edge-preserving, and noise-reducing smoothing filter for images. It replaces the intensity of each pixel with a weighted average of intensity values from nearby pixels. This weight can be based on a Gaussian distribution. Crucially, the weights depend not only on Euclidean distance of pixels, but also on the radiometric differences (e.g., range differences, such as color intensity, depth distance, etc.). This preserves sharp edges.

$$I'(u) = \frac{\sum_{p \in N(u)} e^{-\frac{\|u-p\|^2}{2\sigma_c^2}} e^{-\frac{|I(u)-I(p)|}{2\sigma_s^2}} I(p)}{\sum_{p \in N(u)} e^{-\frac{\|u-p\|^2}{2\sigma_c^2}} e^{-\frac{|I(u)-I(p)|}{2\sigma_s^2}}}$$

where

$\sigma_c$  and  $\sigma_s$  are parameters controlling the fall-off of weights in spatial and intensity domains, respectively,  $N(u)$  is a spatial neighborhood of pixel  $I(u)$ .

## 2.4 Fuzzy C algorithm

Fuzzy clustering is a form of clustering in which each data point can belong to more than one cluster. Clustering or cluster analysis involves assigning data points to clusters such that items in the same cluster are as similar as possible, while items belonging to different clusters are as dissimilar as possible. Clusters are identified via similarity measures. These similarity measures include distance, connectivity, and intensity. Different similarity measures may be chosen based on the data or the application.

## 3 RESULTS AND ANALYSIS

### 3.1 GUI window

GUI is created using a matlab as a dialog box as shown in the fig-3, which has 3 different column ,1<sup>st</sup> column display the input images, 2<sup>nd</sup> column shown the position of sun and 3<sup>rd</sup> column shows the visibility of the sun. Also GUI consist of slide bar to move on to the next slide.



**Fig -3:** GUI dialog box

Image processing is shown in fig-4, based on the image displayed in 1<sup>st</sup> column , 2<sup>nd</sup> column will display whether it is forenoon (6am), noon (12pm), afternoon (3pm) and evening (5pm). Then the 3<sup>rd</sup> column will display either Solar irradiance is Maximum or Sun is invisible with Cloud. Also helps to move one image to another image.



**Fig -4:** Sun position identification

## 4 CONCLUSION

This project has reviewed the state of the art in solar forecasting, and examined the challenges that the world's electrical grids are facing from the rise of solar power levels. It shows the use of image based solar short-term solar forecasting is widely useful for a range of solar power applications, and specifically, that it can help solve the problem of solar intermittency on electrical grids and mini grids by enabling predictive control of loads and generation.

## 5 REFERENCES

- [1]. Badescu, V. (2008) 'Modeling Solar Radiation at the Earth Surface', Berlin Heidelberg: Springer-Verlag.
- [2]. Bernecker, D. Riess, C. Angelopoulou, E. and Hornegger, J. (2014) 'Short-term irradiance forecast using sky images', *Solar Energy*, vol. 110, pp.303–315.
- [3]. Chu, Y. Pedro, H. T. C. and Coimbra, C.F.M. (2013) 'Hybrid intra-hour DNI forecasts with sky image processing enhanced by stochastic learning', *Solar Energy*, vol. 98, part C, pp.592–603.
- [4]. Chu, Y. Pedro, H.T.C. Inman, R.H. and Coimbra, C.F.M. (2014) 'A smart image-based cloud detection system for intra hour solar irradiance forecasts', *J. Atmos. Oceanic Technol.*, vol. 31, no.9, pp.1995–2007.
- [5]. Chow, C.W. Urquhart, B. Lave, M. Dominguez, A. and Washom, B. (2011), 'Intra-hour forecasting with a total sky imager at the UC San Diego solar energy test bed', *Solar Energy*, vol. 85, no. 11, pp.2881-2893.
- [6]. Ineichen, P. and Perez, R. (2002) 'A new air mass independent formulation for the Link turbidity coefficient', *Solar Energy*, vol. 73, no. 3, pp. 151–157.
- [7]. Marquez, R. Pedro, H.T.C. and Coimbra, C.F.M (2013) 'Hybrid solar forecasting method uses satellite imaging and ground telemetry as inputs to ANNs', *Solar Energy*, vol. 92, pp. 176–188.
- [8]. Perez, R. Ineichen, P. Moore, K. and Vignola, F. (2002) 'A new operational model for satellite-derived irradiances: description and validation', *Solar Energy*, vol. 73, no. 5, pp. 307–317.
- [9]. Perez, R. Ineichen, P. Kmiecik, M. Moore, K. Renne, D. and George, R. (2004) 'Producing satellite-derived irradiances in complex arid terrain', *Solar Energy*, vol. 77, no. 4, pp.367–371.
- [10]. Quesada-Ruiz, S. Chu, Y. Tovar-Pescador, J. Pedro and, H.T.C. Coimbra, C.F.M. (2014) 'Cloud tracking methodology for intra-hour {DNI} forecasting', *Solar Energy*, vol.102, pp.267–275.
- [11]. Systems, Y.E. (2012) 'TSI-880 Automatic Total Sky Imager', Airport Industrial Park 101 Industrial Blvd. Turners Falls, MA 01376 USA.
- [12]. West Rowe, S.R. Sayeef, D. and Berry, A. (2014) 'Short term irradiance forecasting using sky cams: Motivation and development', *Solar Energy*, vol. 110, pp.188–207.